29th EPS Conference on Plasma Phys. and Contr. Fusion Montreux, 17-21 June 2002 ECA Vol. **26B**, P-5.072 (2002)

A Low–Frequency Electromagnetic Wave Propagation Code in 2D and 3D

P.Popovich, W.A.Cooper, L.Villard

Centre de Recherches en Physique des Plasmas,
Association EURATOM - Confédération Suisse, EPFL, 1015 Lausanne, Switzerland

The studies of the 3D plasma perturbations in the low-frequency domain (ICRF and shear Alfvén waves, both continuum part of the spectrum and discrete eigenmodes) have received considerable interest lately because of their potential importance for plasma heating, stability and current drive in stellarators [1, 2]. While analytical analysis of low-frequency global oscillations of plasma is still possible for relatively simple geometries, numerical solutions are required for a realistic fully 3D stellarator geometry with inhomogeneous plasma. We are developing a code LEMan for modeling low-frequency electromagnetic wave propagation in inhomogeneous 3D plasmas of a finite spatial extent, including the effects of absorption of the incident wave, reflection from the walls, etc. This requires the solution of the full wave equation. The equation is formulated in terms of the vector and scalar electromagnetic potentials $(\overrightarrow{A}, \phi)$:

$$\begin{cases} \nabla^2 \overrightarrow{A} + k_0^2 \hat{\epsilon} \cdot \overrightarrow{A} + i k_0 \hat{\epsilon} \cdot \nabla \phi &= -\dfrac{4\pi}{c} \overrightarrow{j}_{ext} \\ \nabla \cdot (\hat{\epsilon} \cdot \nabla \phi) - i k_0 \nabla \cdot (\hat{\epsilon} \cdot \overrightarrow{A}) &= -4\pi \rho_{ext} \end{cases} \tag{1}$$

This choice of the formulation guarantees that, applying standard finite elements, the solution is free from the numerical pollution [3]. The underlying equilibrium is obtained numerically with the ideal MHD VMEC code [4], presuming a nested toroidal flux geometry. This equilibrium is then treated in the TERPSICHORE code [5]. TERPSICHORE recalculates all the equilibrium quantities (metric elements, magnetic field components) in the Boozer magnetic coordinate frame [6]. The wave equation (1) is formulated as a variational principle best suited for discretization with finite elements:

$$\begin{cases} \int_\Omega dV \left[-(\nabla \times \overrightarrow{F}) \cdot (\nabla \times \overrightarrow{A}) - (\nabla \cdot \overrightarrow{F})(\nabla \cdot \overrightarrow{A}) + k_0^2 \overrightarrow{F} \cdot (\hat{\epsilon} \cdot \overrightarrow{A}) + i k_0 \overrightarrow{F} \cdot (\hat{\epsilon} \cdot \nabla \phi) \right] \\ \qquad + \int_{\delta\Omega} \overrightarrow{dS} \cdot \left[\overrightarrow{F} \times \nabla \times \overrightarrow{A} + \overrightarrow{F} (\nabla \cdot \overrightarrow{A}) \right] = -\dfrac{4\pi}{c} \int_\Omega dV \overrightarrow{F} \cdot \overrightarrow{j}_{ext} \\ \int_\Omega dV \left[\nabla G \cdot (\hat{\epsilon} \cdot \nabla \phi) - i k_0 \nabla G \cdot (\hat{\epsilon} \cdot \overrightarrow{A}) \right] + \int_{\delta\Omega} \overrightarrow{dS} \cdot \left[i k_0 G \, \hat{\epsilon} \cdot \overrightarrow{A} - G \, \hat{\epsilon} \cdot \nabla \phi \right] \\ \qquad = -4\pi \int_\Omega dV G \rho_{ext}, \end{cases}$$

where $(\overrightarrow{F}, G)$ are test functions, $k_0 = \omega/c$.

The integration over the whole volume of plasma and vacuum (pseudosurfaces) is implied. This approach simplifies the implementation of the vacuum region — numerically, the only difference between vacuum and plasma is the dielectric tensor $\hat{\epsilon}$. For the plasma-wave interaction description, the classical cold plasma model has been implemented. This model includes the effects of finite electron mass, thus the parallel component of the electric field. This allows for the modeling of the mode-conversion effects. The vector potential is written as a sum of a normal, binormal and parallel components, that, along

with the scalar potential, are the actual unknowns of the equation. Such a choice of the unknowns largely simplifies the boundary conditions, that otherwise could have been very complicated in a realistic 3D stellarator configuration. Plasma perturbations are excited with an external antenna. The antenna is modeled numerically by specifying the volume density of external sources of current $\vec{j}_{ext}$ and charge ρ_{ext} in the vacuum or inside the plasma. Fourier decomposition in toroidal and poloidal angles is then applied, combined with finite elements in the radial direction. This approach may prove to be particularly efficient for the case of Alfvén waves, because the condition of the Alfvén resonance and mode conversion is satisfied on the magnetic surfaces [7] (at least in axisymmetric configurations), and the number of the Fourier modes needed to describe the solution in this case may be relatively small. Linear finite elements are sufficient for the discretisation of the cold plasma dielectric tensor because it does not include any differential operators. But linear elements may still be a cause of bad convergence near the magnetic axis. The analytical investigation of the equation has shown that certain Fourier components of the potentials have diverging derivatives on the axis. This deteriorates the convergence of the scheme, because integrals in the variational form containing these derivatives diverge logarithmically. This has partly been avoided by replacing the first finite element with a modified one that corresponds to the asymptotics of the solution. This method has considerably improved the convergence. For example, the proper eigenfrequencies of vacuum cavity oscillations that converged linearly with the standard linear finite elements have close to quadratic convergence with the new modified elements.

The full wave equation with a given antenna excitation entirely defines the solution, which in our case is the set of perturbed vector and scalar potentials. All the other quantities such as EM fields and power fluxes are calculated from the potentials. These diagnostics can also be used for the self-consistency verification of the solution, namely to evaluate the energy conservation. The total power absorbed in the plasma between the magnetic axis and the magnetic flux surface labeled s should be equal to the inward power flux through this surface plus the power coupled in the antenna inside this surface:

$$P_{plasma}(s) = iS_{flux}(s) + P_{ant}(s)$$

The real part of this relation corresponds to the reactive power, and the imaginary part is the resistive power. The classical cold plasma dielectric tensor does not include resistivity, but we modeled it by introducing a small imaginary part in the frequency. A convergence study in a low aspect ratio ($R/a = 5$) 2D geometry has shown linear dependence of the maximum discrepancy in the powers (in the local power balance) on the mesh step. The global power balance has been much easier to satisfy in all the cases analysed.

An important test of the code in the geometry allowing an analytical solution has been an analysis of the oscillation spectrum of a cold plasma cylindrical plasma column. Different modes have been studied — global eigenmodes of the Alfvén wave, local Alfvén resonances (continuum), fast magnetosonic waves for several poloidal mode numbers. The structure of the modes obtained with the global code in the large aspect ratio limit agrees with the analytical solution, which is known for constant plasma density profile in the limit of zero electron mass and low frequency [8]. There is no analytical solution in the

general case of arbitrary density profile with poloidal magnetic field, but the positions of resonant Alfvén surfaces can still be calculated, and they are in a good agreement with the LEMan code results.

A more complicated configuration has been used to test the code in the 2D geometry. A comparison of modes structure in a realistic tokamak configuration between the LEMan code and the LION code [9] has been made. The positions of the local Alfvén resonances are in a good agreement with the LION calculations, forming a gap in frequencies near the $q = 1.5$ surface, which is a very characteristic toroidal effect. The gap (fig 1.) is formed near the crossing of two cylindrical branches of the Alfvén continuum ($n = 1$, $m = -1, -2$) because the symmetry is broken in the poloidal direction, and different poloidal modes couple.

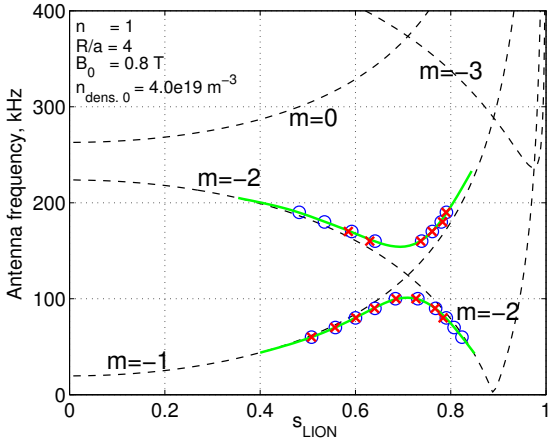

Figure 1. *The structure of the Alfvén continuum near the gap. Dotted lines — cylindrical modes, solid lines — approx. positions of the modes in toroidal geometry, circles — LION code calculations, crosses — LEMan results.*

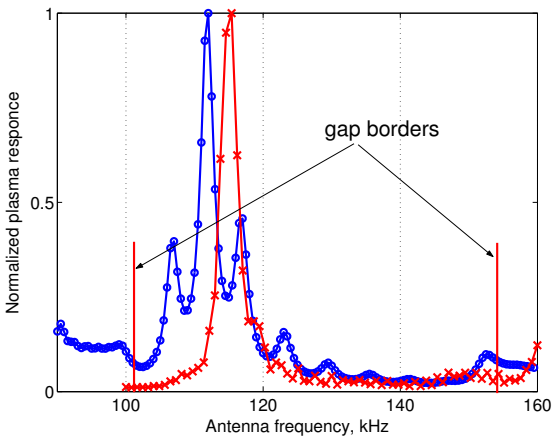

Figure 2. *Frequency scan in the gap region. Circles — LION code, crosses — LEMan results.*

The corresponding wavefields show similar behaviour in both codes, apart from the expected effects due to the difference in physical models (different dielectric tensors). The LION code uses an approximation of zero electron mass, hence the parallel component of the electric field vanishes and the fields become singular on the resonant surface (at zero resistivity). An inclusion of the finite electron mass in the tensor results in the appearance of short wavelength oscillations propagating from the Alfvén resonance — the mode conversion effect. A frequency scan in the region of the gap reveals the presence of a discrete mode. Both the LEMan code and LION show a peak in plasma response (total power coupled in the antenna) within less than 3% difference in frequency (fig. 2). The peak corresponds to the toroidicity induced Alfvén eigenmode (TAE). The discrepancy in frequency can be explained by slight difference in the equilibrium, produced by different codes (VMEC and CHEASE). This is a strong test of the toroidal structure of the new code, because the presence of the gap and the TAE are purely toroidal effects. A comparison of Alfvén resonant surface positions between LION and LEMan has been also made for a series of Soloviev equilibria. Using analytical equilibria allows us to avoid the numerical imprecisions of the equilibrium code. All these tests have shown a good one-to-one correspondence between the results.

Many Alfvén modes already exist in tokamak geometry. However, the "zoo" of the possible modes becomes much more diverse in the fully three dimensional configurations [10]. In 3D, the symmetry is broken both in poloidal and toroidal directions, so not only poloidal, but also toroidal modes can be coupled. Even with a relatively simple cold plasma dielectric model the structure of the wavefields in a realistic stellarator configuration is very hard to analyse because of the coupling between different poloidal and toroidal modes. In order to test the 3D structure of the code, at the same time keeping the spectrum of modes relatively simple, we have taken a mirror-like two period configuration with large aspect ratio ($R/a = 10^2$).

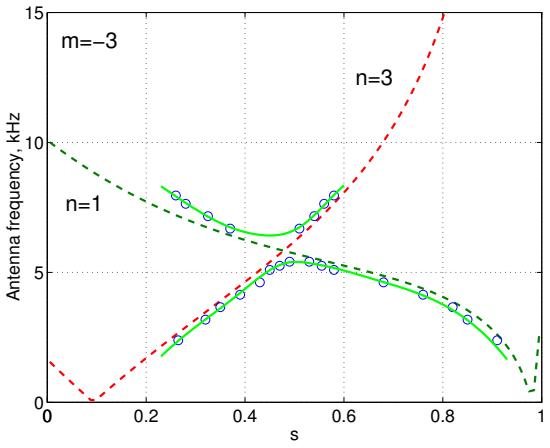

Figure 3. *The structure of the Alfvén continuum near the mirror-induced gap. Dotted lines — cylindrical modes, solid lines — approx. positions of the modes in the mirror geometry.*

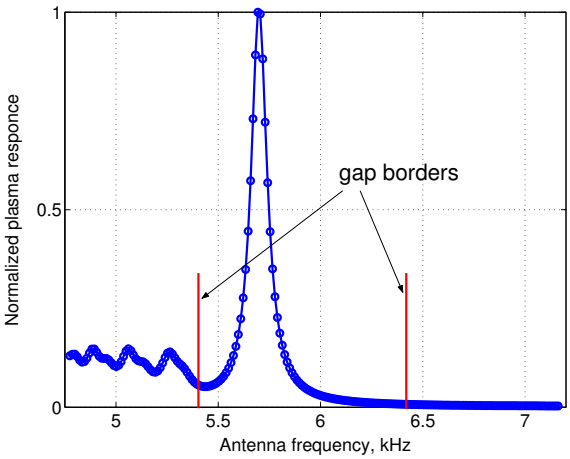

Figure 4. *Frequency scan in the gap region.*

Because of the periodicity, only modes with $n - n' = kN$ are coupled, where N is the number of periods and k — any integer. Analogously to the toroidal coupling in tokamak, the mirror-induced coupling of modes with different n results in the formation of a gap near the crossing of the cylindrical branches of the Alfvén continuum (fig 3). The plasma response as a function of antenna frequency has a peak inside the gap that can be explained by a presence of a mirror-induced Alfvén eigenmode (MAE) (fig 4).

References

[1] E. F. Jaeger, L. A. Berry, E. D'Azevedo, D. B. Batchelor, M. D. Carter, and K. F. White, Phys. of Plasma 9(5) (2002) 1873
[2] V.Vdovin, T.Watari, A.Fukuyama, Proc. ICPP 96 (Nagoya 1996),1070; NIFS-469 L.
[3] A. Jaun, K. Appert, J. Vaclavik, L. Villard, Comp. Phys. Comm. 92, 153 (1995)
[4] S.P. Hirshman, U. Schwenn and J. Nührenberg, J. Comput. Phys. 87, 396 (1989)
[5] D.V. Anderson, W.A. Cooper, R. Gruber, S. Merazzi and U. Schwenn, The International Journal of Supercomputer Applications 4, 34 (1990)
[6] A. Boozer, Phys. Fluids 23(5), 904 (1980)
[7] E. Tennfors, Plasma Phys. Contr. Fus. 28 (1986) 1483
[8] K. Appert, J. Vaclavik, L. Villard, Phys. Fluids 27 (2), 1984
[9] L. Villard, K. Appert, R. Gruber, J. Vaclavik, Comput. Phys. Reports 4 (1986) 95
[10] Ya. I. Kolesnichenko, V. V. Lutsenko Phys. of Plasmas 8(2), 491 (2001)